Appl. Phys. A 74 [Suppl.], S1635–S1637 (2002) / Digital Object Identifier (DOI) 10.1007/s003390201933

Applied Physics A
Materials
Science & Processing

Lattice and charge effects in high-temperature superconductors

T. Egami[1,*], R.J. McQueeney[2], J.-H. Chung[1], M. Yethiraj[3], H.A. Mook[3], M. Arai[4], Y. Inamura[4], Y. Endoh[5], S. Tajima[6], C. Frost[7], F. Dogan[8]

[1] Laboratory for Research on the Structure of Matter and Department of Materials Science and Engineering, University of Pennsylvania, Philadelphia, PA 19104-6272 USA
[2] Los Alamos National Laboratory, Los Alamos, NM 87545 USA
[3] Oak Ridge National Laboratory, Oak Ridge, TN 37831, USA
[4] Institute of Materials Structure Science, KEK, Tsukuba 305-0801, Japan
[5] Institute for Materials Research, Tohoku University, Sendai 980, Japan
[6] Superconductivity Research Laboratory, International Superconductivity Technology Center, Tokyo 135-0062, Japan
[7] Rutherford Appleton Laboratory, Didcot, Oxon, OX11 0QX, UK
[8] Department of Materials Science, University of Washington, Seattle, WA 98195, USA

Received: 13 July 2001/Accepted: 31 August 2002 –

Abstract. We present the results of inelastic neutron-scattering measurements of a twinned crystal of $YBa_2Cu_3O_{6.95}$ using the MAPS spectrometer of the ISIS facility of the Rutherford–Appleton Laboratory as well as the HFIR of the Oak Ridge National Laboratory. The dispersion of the Cu–O bond-stretching modes indicates a strong dielectric anisotropy within the plane and associated electronic anisotropy, supporting the dynamic stripe model. The results suggest a possibility that phonons play a major role in the mechanism of high-temperature superconductivity.

PACS: 63.20.-e; 74.72.-h; 78.70.Nx

Phonons are generally considered to be irrelevant, or even harmful, to the high-temperature superconductivity (HTSC) in the cuprates. This is because the critical temperature appears to be too high for the BCS mechanism, the isotope effect is small, there is no evidence of strong electron–phonon interaction in the normal-state transport properties, and the attractive phonon mechanism for pair formation appears to compete against the repulsive magnetic mechanism [1]. However, there are a number of indications that phonons are playing some active role in the HTSC phenomenon [2, 3]. Also, the electron–phonon coupling in strongly correlated electron systems can be very different, being strongly dependent upon the momentum and energy, so that the conjecture based upon the conventional electron–phonon interaction may not be valid for the cuprates [2]. In this paper we present the results of our inelastic neutron scattering measurements on a twinned crystal of $YBa_2Cu_3O_{6.95}$ (YBCO) that support this view [4]. We found that the dispersion of the Cu–O bond-stretching mode is strongly anisotropic in the CuO_2 plane, suggesting strong in-plane dielectric anisotropy in the phonon-frequency range. The results support the spin/charge stripe model, and strongly challenge the conventional view of the role of phonons in the mechanism of HTSC.

*Corresponding author.
(Fax: +1-215/573-2128, E-mail: egami@seas.upenn.edu)

1 Experimental results

For a long time the standard method of determining the phonon dispersion was an inelastic neutron scattering measurement using a triple-axis-spectrometer. With this method the relation between $\boldsymbol{Q}$, the momentum transfer, and ω, the energy transfer, is determined point-by-point in a serial manner. A modern time-of-flight chopper spectrometer for a pulsed neutron source, such as MAPS of the ISIS facility of the Rutherford–Appleton Laboratory, is equipped with a large array of detectors that enable parallel counting of neutrons. Thus the dynamical structure factor, $S(\boldsymbol{Q}, \omega)$, covering a large $\boldsymbol{Q}$-ω space is determined simultaneously in a three-dimensional space (energy and two axes of momentum transfer). For instance, the MAPS is equipped with nearly 700 position-sensitive ^{3}He neutron detectors covering 16 m^2, which results in the total number of pixels of approximately 1.5×10^5 and the time channel of 10^3. In a typical measurement over 24 h many phonon branches are observed at once, while it would take many days to do the same with the triple-axis spectrometer. The raw data were mapped into $S(\boldsymbol{Q}, \omega)$ and various two-dimensional projections were produced by the Mslice software.

The sample we studied using MAPS was a crystal of $YBa_2Cu_3O_{6.95}$ ($T_C = 93$ K) produced by flux growth in the shape of a disk, weighing about 100 g [5]. The crystal was twinned with equal shares. The sample was placed in a Displex closed-cycle refrigerator with the a/b axis in the vertical position and the c axis away from the incident beam by 41° in the horizontal plane. The incident energy was chosen to be 117.5 meV with the resolution of 5 meV for the elastic peak and 3 meV at 60-meV energy transfer. The data were taken over 24 h for each run. As an example the cut of $S(\boldsymbol{Q}, \omega)$ at a constant energy transfer of 41 meV (integrated from 40 to 42 meV) is presented in Fig. 1. The data nominally represent $S(\boldsymbol{Q}, \omega)$ taken at $T = 7$ K in the h-k plane, while l is actually varying with ω. Here h, k, l are in units of the reciprocal lattice vectors, and the data were processed by subtracting the energy-dependent background (typically 40%) and dividing it by Q^2 to represent the phonon intensity. In YBCO the

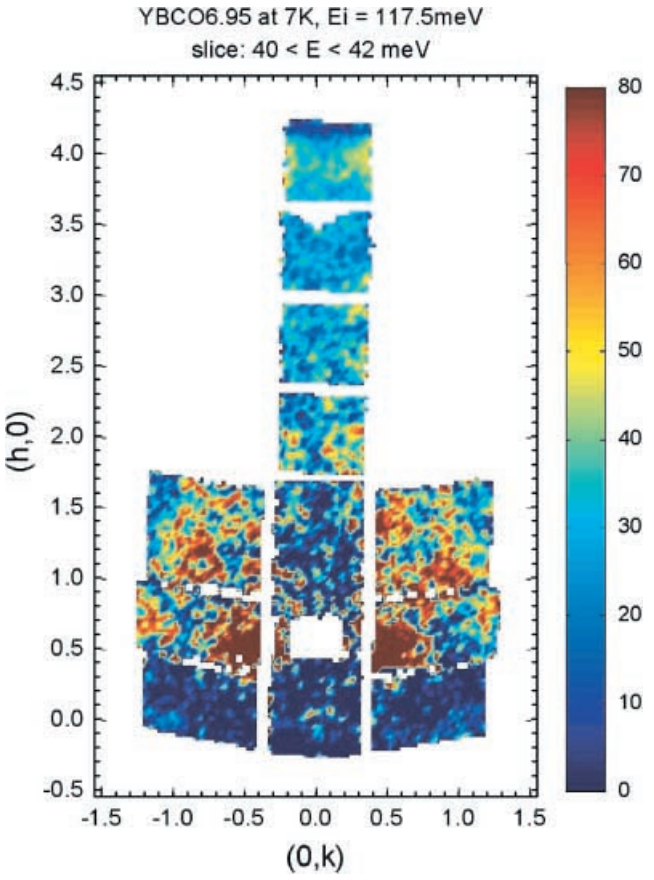

Fig. 1. $S(\mathbf{Q}, \omega)$ of YBCO at $T = 7$ K cut at 41 meV (summed between 40 and 41 meV), projected on the h-k plane. *White lines* are due to gaps in detector coverage. The data were divided by Q^2 after subtracting the background. Magnetic scattering peaks are seen at $(0.5, \pm 0.5)$

l dependence is weak because of the layered nature, so it is neglected for the moment in the present analysis, and below only (h, k) indices will be used. In addition to the magnetic scattering around $(0.5, \pm 0.5)$ many areas with high intensity due to phonon modes are seen.

Figure 2 is a cut along h at $k = 0$ (integrated over $-0.1 < k < 0.1$) that shows $S(\boldsymbol{Q}, \omega)$ in the h-ω plane, for the $T = 110$ K data. Note that in the neutron inelastic scattering the scattered intensity at the momentum transfer $\boldsymbol{Q}$ is proportional to $(\boldsymbol{Q} \cdot \boldsymbol{\varepsilon})^2$, where $\boldsymbol{\varepsilon}$ is the phonon polarization. Thus in this cut we see only the longitudinal modes, since the phonon momentum, $\boldsymbol{Q} = \boldsymbol{Q} - \boldsymbol{K}$, where $\boldsymbol{K}$ is the reciprocal lattice vector, is parallel to $\boldsymbol{Q}$, and therefore to $\boldsymbol{\varepsilon}$. We at first focused on the high-energy Cu–O bond-stretching LO modes, since the change in the Cu–O distance induces charge transfer between Cu and O; the electron–phonon interaction is expected to be very strong for this mode, particularly at the zone edge [6]. Anomalous behaviors were observed for this mode in $La_{2-x}Sr_xCuO_4$ (LSCO) [7, 8]. The incident energy and the orientation of the sample were chosen in such a way that the l index for this mode is about 2, corresponding to Q_z of about $1\,\text{Å}^{-1}$ at 70 meV, so that the observed modes are antisymmetric about the two CuO_2 planes in YBCO, which are separated by 3.2 Å. At the energy transfer of 50 meV the l index is zero, so that only the symmetric mode is observed.

Surprisingly and luckily, we were able to differentiate the LO mode propagating along the a from that along the b directions, since the lattice constants are different by 2% due to orthorhombicity and the energy was also different by 5 meV at the zone center. In Fig. 2 it is possible to identify a mode near (3, 0) that has a maximum energy of 72 meV around (3.02, 0). Even though the Q resolution is 0.05, by peak fitting the point of reflection symmetry was fairly accurately determined. Since we assumed tetragonal symmetry and used a provisional lattice constant of 3.84 Å in Fig. 2, this means that the actual lattice constant for this mode is 3.82 Å, which is close to the lattice constant a. Thus this mode must be propagating along the a axis (perpendicular to the chain) with the polarization also along a. The other mode has the energy of 67 meV at the maximum around (2.96, 0), corresponding to the actual lattice constant of 3.88 Å, suggesting that this is the b-axis mode. The Raman data on a detwinned sample [9] are in full agreement with the energies at the zone centers of the orthorhombic zone, 72 meV at (3, 0) and 67 meV at (0, 3), yielding the identification as the B_{2g} and B_{3g} modes, respectively.

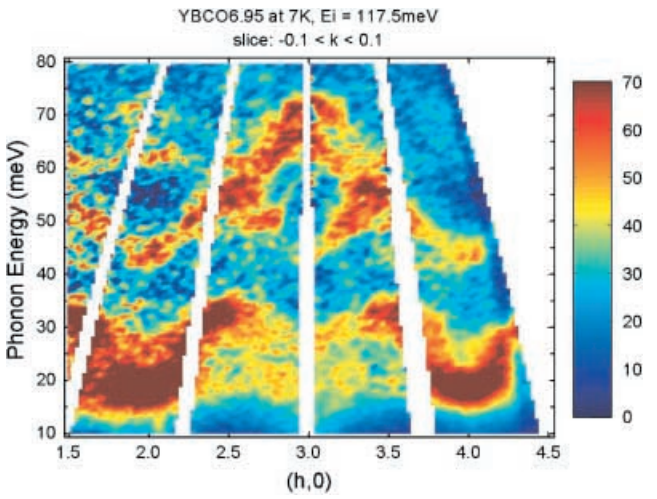

Fig. 2. $S(\mathbf{Q}, \omega)$ of YBCO at $T = 110$ K, cut along the h-ω plane. Data were divided by Q^2 after background subtraction. Several LO and LA phonon branches are seen

We also made a cut along k at $h = 3.0$ to observe the transverse (TO) modes. In the k-ω cut including the zone center the phonon momentum q is nearly perpendicular to $\boldsymbol{Q}$, so only the TO modes are observed. Due to the limited range of the detector position only the portion of k from -0.25 to 0.25 could be observed for the present setting. The dispersion thus determined is shown in Fig. 3. The mode with the polarization along $\boldsymbol{b}$ (chain direction), denoted as B_{3g} at the zone center, has normal dispersion. The LO and TO modes are almost degenerate, consistent with metallic screening of local dipoles. However, the mode along $\boldsymbol{a}$, B_{2g} at the zone center, shows an anomalous behavior just like LSCO [7]. The LO branch has a large jump at the middle of the zone (0.25, 0), and the TO energy is higher than the LO energy except for $q = 0$. This conspicuous difference between the modes with polarization along $\boldsymbol{a}$ and $\boldsymbol{b}$ suggests strong dielectric anisotropy in the CuO_2 plane: the modes are screened strongly along $\boldsymbol{b}$, but not so much along $\boldsymbol{a}$. Another measurement done at $T = 7$ K shows that even the B_{3g} mode has a gap in the intensity around (0.25, 0). Additional data were obtained with the triple-axis spectrometer, HB-3, of the HFIR of the Oak Ridge National Laboratory. For the triple-axis measurements the fi-

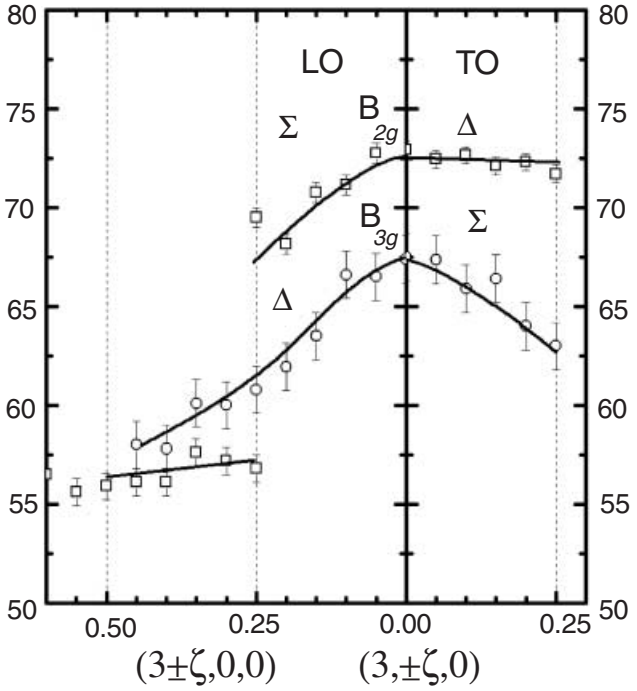

Fig. 3. Dispersion of the LO (*left*) and TO (*right*) Cu–O bond-stretching modes. The branch labeled B_{2g} at the zone center has the polarization along a (perpendicular to the chain), while the B_{3g} mode has the polarization along b. Due to the limited range of detector positions TO was observed only up to $k = 0.25$. The dispersions are corrected for the shifts due to the difference in the lattice constants a and b

nal energy was fixed at 14.87 meV and the sample-to-detector horizontal collimation elements were 48′–60′–40′–120′. The temperature dependence of this change in the phonon intensity at (0.25, 0) studied at the HIFIR indicates that the change occurs only below T_C, and is closely connected to the superconducting order parameter. Thus the gap in the dispersion of the LO mode develops from one dimension at high temperatures to two dimensions in the superconducting phase.

2 Discussion

The gap in the dispersion of the LO mode along $\boldsymbol{a}$ at (0.25, 0) is very similar to the one observed for LSCO [7], and suggests possible cell doubling in the a direction, but not in the b direction. The simplest interpretation of this anisotropy is to invoke the stripe model [10] in which the charge stripe is along the b axis [11]. The period of the stripe, however, must be $2a$, rather than $4a$ as in the standard model. Also, formation of the stripes must be short-range and dynamic, since the superlattice diffraction has never been observed. The dispersion may be modeled as the response of the dynamic charge stripes, which are in resonance with the phonon forming a vibronic state [12]. The possible role of the vibronic state has been advocated for a long time by Goodenough [13]. Usually the dielectric response of electrons increases the LO frequency, as in many insulating dielectric solids and described by the Lyddane–Sachs–Teller (LST) equation. However, here the LO frequency is lower than the TO frequency, suggesting an inverse LST relationship. Physically the inverse LST relationship means that the lateral vibration of the charge stripes is out of phase with the phonon, creating the overscreened state. Overscreening must be short-range, since it is not happening at $q = 0$. Such overscreening turns electron repulsion into attraction, and can contribute to the pairing mechanism [12].

Since the electron–phonon interaction due to this mode is highly directional, mainly along the [100] direction, in the case of the d-wave superconductivity the phonon mechanism is not in conflict with the magnetic mechanism, which is repulsive along [110]. It is interesting to note that this mechanism produces a supercurrent mainly in the direction perpendicular to the stripes, while many one-dimensional stripe models [14] create the supercurrent mainly along the stripes. The recent ARPES result [15] appears to favor the former, while it is still inconclusive since the size of the gap seems to be larger in the direction along the stripes.

This mechanism overlaps with other phonon mechanisms [16–18] and it is too early to fully assess the implication of the present observation. But it is clear that the present results suggest the importance of the charge channel to the pairing mechanism through dielectric interactions, and strongly challenge the majority view in the field that the phonons and charge fluctuations are irrelevant to the HTSC phenomena.

Acknowledgements. The authors are grateful to M. Tachiki, S. Sachdev, T. Perring and J.C. Phillips for useful discussions. The work was supported by the National Science Foundation through DMR96-28134 and DMR01-02565.

References

1. P.W. Anderson: *Theory of Superconductivity in the High-T_C Cuprates* (Princeton University Press, Princeton 1997)
2. T. Egami, S.J.L. Billinge: In *Physical Properties of High Temperature Superconductors V*, ed. by D. Ginsberg (World Scientific, Singapore 1996) p. 265
3. L. Pintschovius, W. Reichardt: In *Physical Properties of High Temperature Superconductors IV*, ed. by D. Ginsberg (World Scientific, Singapore 1994) p. 295
4. R.J. McQueeney, T. Egami, J.-H. Chung, Y. Petrov, M. Yethiraj, M. Arai, Y. Inamura, Y. Endoh, S. Tajima, C. Frost, F. Dogan: cond-mat/0105593
5. The crystal is similar to the one described in H.F. Fong, B. Keimer, P.W. Anderson, D. Reznik, F. Dogan, I.A. Aksay: Phys. Rev. Lett. **75**, 316 (1995)
6. S. Ishihara, T. Egami, M. Tachiki: Phys. Rev. B **55**, 3163 (1997)
7. R.J. McQueeney, Y. Petrov, T. Egami, M. Yethiraj, G. Shirane, Y. Endoh: Phys. Rev. Lett. **82**, 628 (1999)
8. R.J. McQueeney, J.L. Sarrao, P.G. Pagliuso, P.W. Stephens, R. Osborn: Phys. Rev. Lett. **87**, 077 001 (2001)
9. K.F. McCarty, J.Z. Liu, R.N. Shelton, H.B. Radousky: Phys. Rev. B **41**, 8792 (1990)
10. J.M. Tranquada et al.: Nature **375**, 561 (1995)
11. H.A. Mook, P. Dai, F. Dogan, R.D. Hunt: Nature **404**, 729 (2000)
12. M. Tachiki, S. Takahashi: Phys. Rev. B **39**, 293 (1989).
13. e.g., J.B. Goodenough, J.-S. Zhou: In *Stripes and Related Phenomena* ed. by A. Bianconi, N.L. Saini (Kluwar Academic/Plenum Pub., New York 2000) p. 199
14. e.g., S.A. Kivelson, E. Fradkin, V.J. Emery: Nature (London) **393**, 550 (1998)
15. D.H. Lu, D.L. Feng, N.P. Armitage, K.M. Shen, A. Damascelli, C. Kim, F. Ronning, Z.-X. Shen: Phys. Rev. Lett. **86**, 4370 (2001)
16. A. Bussmann-Holder, A. Müller, R. Micnas, H. Büttner, A. Simon, A.R. Bishop, T. Egami: J. Phys. Condens. Matter **13**, L169 (2001)
17. E.W. Carlson, D. Orgad: Phys. Rev. B **62**, 3422 (2000)
18. A.H. Castro-Neto: J. Superconductivity **13**, 913 (2000); cond-mat/0102281